Food Chemistry: X 19 (2023) 100794

Contents lists available at ScienceDirect

Food Chemistry: X

journal homepage: www.sciencedirect.com/journal/food-chemistry-x

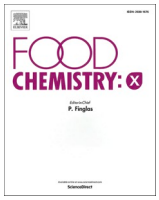

Determination of procymidone residues in rapeseed oil based on olfactory visualization technology

Hui Jiang [a,*], Mingxing Zhao [a], Quansheng Chen [b,*]

[a] School of Electrical and Information Engineering, Jiangsu University, Zhenjiang 212013, China
[b] College of Ocean Food and Biological Engineering, Jimei University, Xiamen 361021, China

ARTICLE INFO

Keywords:
Rapeseed oil
Pesticide residues
Olfactory visualization technology
Feature optimization
Quantitative analysis

ABSTRACT

A new means about olfactory visualization technique for the quantitative analysis of procymidone residues in rapeseed oil has been proposed. First, an olfactory visualization system was set up to collect volatile odor information from rapeseed oil samples containing different concentrations of procymidone residues. Then, we utilized four intelligent optimization algorithms, namely particle swarm optimization (PSO), genetic algorithm (GA), ant colony optimization (ACO) and simulated annealing (SA), to optimize the characteristics of the sensors. Finally, support vector machine regression (SVR) models employing optimized features were constructed for the quantitative detection of procymidone residues in rapeseed oil. The study demonstrated that the SA-SVR model demonstrated superior prediction results, achieving a high determination coefficient of prediction (R_P^2) at 0.9894. As indicated by the results, it is possible to successfully conduct non-destructive detection of procymidone residues in edible oil by the olfactory visualization technology.

1. Introduction

China is an important oil producer and consumer in the world. Among them, rapeseed is the largest oil crop in China, and its planting area and output are increasing annually (Shen et al., 2023). Therefore, rapeseed oil occupies a pivotal position in the supply of edible oil. However, rapeseed, the raw material of rapeseed oil, is often affected by sclerotinia during the planting process, which causes yield loss (Ding et al., 2021). Consequently, pesticides are sprayed during the rapeseed planting process to play a protective role. Procymidone is also known as 2-Cyclopropanedicarboximide. Its chemical formula is $C_{13}H_{11}Cl_2NO_2$, which is a diformimide internal absorption fungicide put into use in the 1970s, inhibits the synthesis of triglycerides in the bacteria, and has the dual effect of protecting and treating rapeseed (Liu et al., 2018). However, with the increasing demand of rapeseed oil, the use of procymidone in production is also increasing, and its residues have also attracted more and more attention. Therefore, it is important to achieve accurate detection of procymidone residues in rapeseed oil.

At present, the detection methods of procymidone residues in grain and oil products mainly include enzyme inhibition, chromatography and immunoassay (Chen, Dong, Xu, Liu, & Zheng, 2015). The enzyme inhibition method can be used for the emergency detection of acute pesticide residues poisoning, but the detection range of this method is small and the sensitivity is low (Katsoudas & Abdelmesseh, 2000). A wide range of mycotoxins can be analyzed with high precision using chromatography, but upfront sample preparation is complex and requires strict operator expertise (Hird, Lau, Schuhmacher, & Krska, 2014). Although the immunoassay method has a rapid detection time, it is not an ideal option for widespread use due to its high cost and complicated preparation process (Garcia-Febrero, Salvador, Sanchez-Baeza, & Marco, 2014). Therefore, an efficient analytical technique is needed to detect procymidone residues in edible oil quickly and on-site.

Olfactory visualization technology is a new type of electronic nose technology. In 2000, Professors Rakow and Suslick proposed to use metalloporphyrins to construct a sensor array to react with the volatile gases of the sample, and qualitatively or quantitatively analyze the color difference of the metalloporphyrin before and after the reaction (Rakow & Suslick, 2000). Compared to traditional electronic nose technology, which relies only on weak van der Waals forces to capture odors, olfactory visualization technology introduces metal bonds and polar bonds to make it more accurate and stable during detection. At the same time, the use of hydrophobic substrates can reduce the influence of ambient humidity on experimental results, and the cost of a single test is low (Suslick, Rakow, & Sen, 2004). Recently, the utilization of olfactory

* Corresponding authors at: School of Electrical and Information Engineering, Jiangsu University, Zhenjiang 212013, China.
E-mail addresses: h.v.jiang@ujs.edu.cn (H. Jiang), chenqs@jmu.edu.cn (Q. Chen).

https://doi.org/10.1016/j.fochx.2023.100794
Received 25 May 2023; Accepted 13 July 2023
Available online 17 July 2023

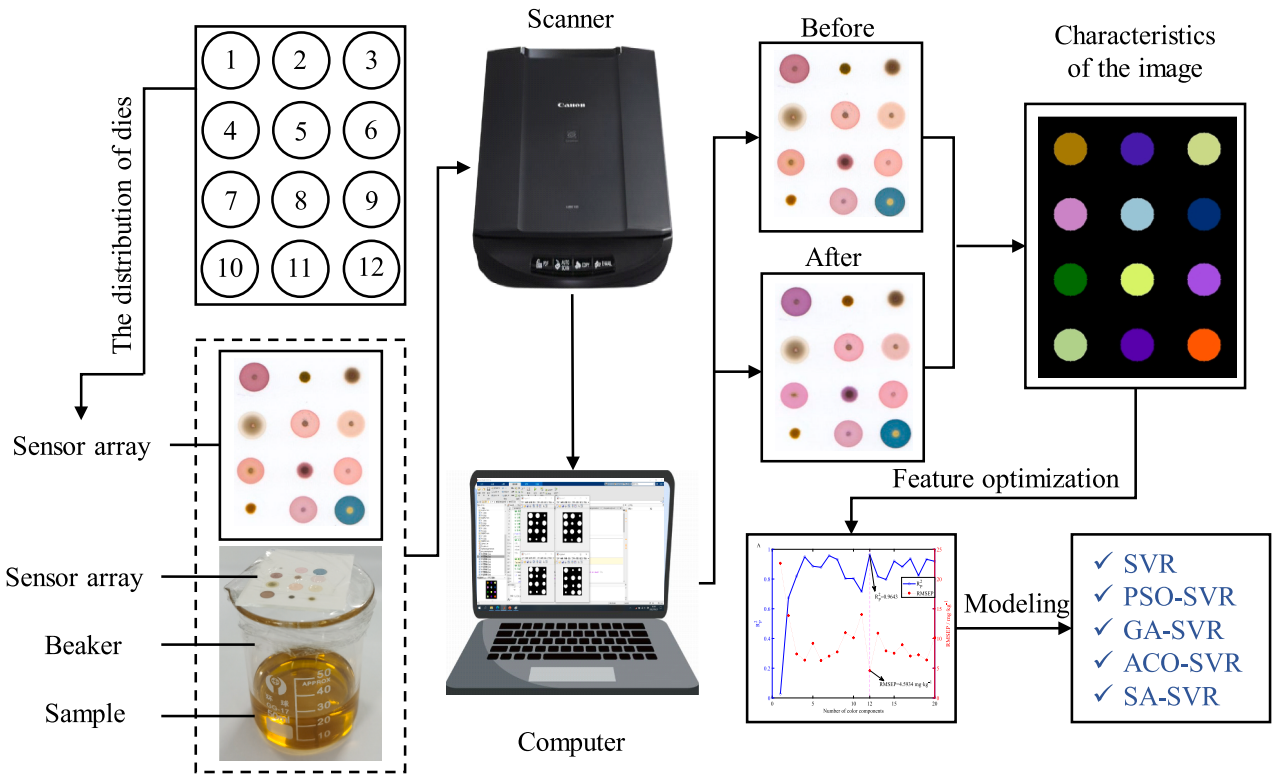

Fig. 1. Schematic diagram of the sensor platform used for quantitative detection of procymidone in rapeseed oil.

visualization technology for detecting hazards in food and agricultural products has become more and more extensive, owing to the advancements in material science (Jiang, Liu, He, & Chen, 2020; Jiang, Xu, & Chen, 2019b; Liu, Jiang, & Chen, 2020; Xu et al., 2022; Zhu, Deng, & Jiang, 2022). Electronic nose technology has also emerged in the detection of pesticide residues in food and agricultural products (Sanaeifar, Li, He, Huang, & Zhan, 2021; Tang et al., 2020; Tang et al., 2021). However, in the detection method of edible oil pesticide residues, there are no documented instances where electronic nose technology has been utilized in literature. Therefore, this study intends to test the feasibility of the novel electronic nose technology (i.e. olfactory visualization technology) for the detection of pesticide residues in edible oil.

Based on the above analysis, the major tasks of this study were organized as shown below. (1) Selected suitable chemical dyes to create a 4 × 3 sensor,which formed an olfactory visualization system; (2) prepared rapeseed oil samples containing different concentrations of procymidone and used the system to collect volatile odor information of the samples by headspace gas enrichment; (3) intelligent optimization algorithms, namely particle swarm optimization (PSO) algorithms, genetic algorithms (GA), ant colony optimization (ACO) and simulated annealing (SA) algorithms, were employed to optimize the characteristic variables; (4) optimization features were utilized to construct support vector machine regression (SVR) models that could quantitatively analyze putrefactive residues in rapeseed oil.

2. Materials and methods

2.1. Sample preparation

The procymidone (analytical standards) and *n*-hexane (≥98.0% (GC)) used in this study were purchased from Shanghai Aladdin. Nine brands of rapeseed oil were purchased from Jingdong mall, namely Caiziwang, Xiancan, Tianfu Oil, Hengli Morgan, DaoDaoquan, Jingchudadi, Fulinmen, Jinlongyu and Luhua.

During sample preparation, we firstly took 200 mg of the procymidone standards and dissolved it in the *n*-hexane solvent. Then we made 16 standard solutions of procymidone in different concentrations. Next, the solutions were diluted with rapeseed oil at a mass ratio of 1:9 (2 g of standard solution and 18 g of rapeseed oil) and ultimately achieved the concentration gradients of the procymidone residues 0.1, 0.2, 0.35, 0.5, 0.6, 0.7, 0.8, 1, 2, 3.5, 6, 7, 8, 10, 50 and 100 mg/kg. There were 9 samples of each concentration gradient and we got 144 samples. After removing 2 abnormal samples, 142 valid samples remained.

2.2. Design of colorimetric sensor array

The effectiveness of olfactory visualization depends on the chemical dyes that are chosen for the sensor array preparation. Chemical dyes generally need to meet the following two conditions: (1) the substance to be tested must display a high level of reactivity with the volatile gases produced; (2) the color should change significantly before and after the chemical dye reaction. Therefore, a total of twelve chemicals were selected, including eleven porphyrins soured from Sigma-Aldrich (USA) and one hydrophobic pH indicator from Sinopharm Group Chemical Reagent Co., Ltd. (Shanghai, China) after several pre-experimental attempts. Basic information on the chemical dyes utilized to prepare the sensor array in this study is shown in Table S1.

Suitable carrier materials have a great influence on the color development reaction of chemical dyes. Carrier materials generally need to meet the following requirements: (1) do not react with color-sensitive materials; (2) provide a uniform white background; (3) have good hydrophobicity. Considering multiple factors, the carrier material chosen for this study was the C_2 reversed-phase silica gel plate from Merck KGaA (USA).

The fabrication processes of the sensor array in this study can be outlined as follows. (1) Each porphyrin compound (4 mg) was dissolved in 2 mL of dichloromethane, and the pH indicator (4 mg) was dissolved in 2 mL of absolute ethanol. The resulting concentration of each solution was 2 mg/mL; (2) sealed the prepared 12 solutions and placed them in

an ultrasonic cleaning machine (model: SB-3200DT, power: 180 W) for 20 min to achieve full dissolution; (3) used spot capillaries (specifications: 0.3 × 100 mm) to drop 12 kinds of configured chemical dyes on the 4 cm × 3 cm C_2 reversed-phase silica gel plate.

2.3. Data acquisition and preprocessing

Fig. 1 depicts the schematic diagram of the sensor platform utilized for detecting procymidone in rapeseed oil. The sensor data collection processes were as follows. (1) Used CanoScan LiDE220 scanner to scan the prepared sensor array in color to obtain the original image of the sensor array; (2) put 20 ± 0.1 g of rapeseed oil sample in a 50 mL glass beaker; (3) fixed the sensor array with tape to the plastic wrap, and then sealed the beaker with the plastic wrap (the chemical dye side faced the rapeseed oil sample and did not come into contact with the sample); (4) placed the beaker at 25 ℃ for 14 min and then used scanner to scan the sensor array in color to obtain images of the reacted sensor array.

The original image and the reactive image of the sensor array acquired by the experiment were preprocessed and the RGB color features were extracted by MATLAB software. The color feature values of the sensor array can be obtained by adding the mean RGB gray values extracted from the reactive image and the original image. Since there are 12 regions of chemical dye on the sensor array, three color signatures (i.e., red, green, blue) can be obtained for each region. This approach enabled each sensor array to acquire 36 distinctive color features.

2.4. Data analyses methods

2.4.1. Particle swarm optimization

Particle swarm optimization (PSO) algorithm, a global search optimization method, is based on swarm intelligence and is also known as the flock system foraging algorithm (Jordehi, 2014). It is established by simulating the characteristics of information sharing between individuals during the foraging process of bird flocks. The algorithm performs optimization iterative calculation according to the speed and position changes of individuals to obtain the optimal solution. Then each particle corresponds to a target fitness value, and each particle has its own flight speed, following the optimal position particle to search the solution space. In the search process, the optimal solution found by each particle during flight is called individual optimal, the optimal solution of all particles in the group is called group optimal, and each particle seeks the optimal position of the individual and the optimal position of the group, so as to ensure that the group finally obtains the optimal target (Jiang, Liu, He, Ding, & Chen, 2021).

In this study, the input feature variables of the model were optimized using PSO. The optimization parameters used in the experiment were as shown below: a maximum iteration of 50, a population size of 20, learning factors of $c_1 = c_2 = 1.4962$, and an inertia weight of 0.7298 with a damping ratio of 1. The algorithm used the root mean square error of prediction (RMSEP) as its fitness function.

2.4.2. Genetic algorithm

Genetic algorithm (GA) is an algorithm borrowed from Darwin's evolutionary model (Niazi & Leardi, 2012). It ultimately achieves the target requirement through selective changes. In the coding space, each individual is a viable solution, called a chromosome. GA continuously updates chromosomes through three stages of selection, crossover, and mutation, and whether the chromosomes meet the requirements needs to be evaluated by the fitness function value. It also introduces the fitness function value to select the next generation in proportion from all current chromosomes. Then enter the loop again, and continue to iterate the calculation until it converges to the global optimal chromosome, that is, the solution needed to solve the trouble (Jiang, Xu, & Chen, 2019a).

In this study, the input feature variables of the model were optimized using GA. The following parameters were used to configure the algorithm: a maximum iteration of 100, a population size of 20, and a crossover probability of 0.7 with a mutation probability of 0.1. The algorithm used the RMSEP as its fitness function.

2.4.3. Ant colony optimization

Ant colony optimization (ACO) is an optimization algorithm that simulates ant colonies to find the optimal path during foraging (Mohan & Baskaran, 2012). Studies have found that when ants move, they rely on the released pheromones to complete information exchange and collaboration between ants, and search towards paths with high pheromone concentration. At the same time, when passing through a path with a high pheromone concentration, it will also release pheromones, resulting in an increasingly high pheromone concentration in the pathway. Finally, the ants of the entire ant colony will follow the path with the highest pheromone concentration to the food source, that is, this path is the optimal path (Tao Liu, He, Yao, Jiang, & Chen, 2022).

In this study, the input feature variables of the model were optimized using ACO. The parameters of the algorithm were set as shown below: the maximum number of iterations was 100, the population size was 20, the initial pheromone concentration was 1, the pheromone evaporation rate was 0.05, the pheromone weight index and the heuristic weight index were 1. The algorithm used the RMSEP as its fitness function.

2.4.4. Simulated annealing

Simulated annealing (SA) is an optimal solution search algorithm based on combinatorial optimization, similar to thermal annealing of solid substances (Suman & Kumar, 2006). It is an optimization algorithm that effectively avoids falling into the local minimum and eventually tends to the global optimal serial structure by giving the search process a time-varying probability burst that eventually tends to zero. SA includes two parts, the Metropolis algorithm and the annealing process, corresponding to the internal cycle and the external cycle. External circulation is to raise the solid to a higher temperature, and then decrease it in a certain proportion with a cooling coefficient. When the termination temperature is reached, the annealing process ends. The internal cycle is iterating several times at each temperature, looking for the minimum value of the energy at that temperature (i.e., the optimal solution) (Mao & Jiang, 2022).

In this study, the input feature variables of the model were optimized using SA. The following parameters were used to configure the algorithm: the maximum number of iterations was 100, the population size was 20, the initial temperature was 10 and the cooling coefficient was 0.99. The algorithm used the RMSEP as its fitness function.

2.4.5. Support vector regression

Support vector regression (SVR) is a specific type of support vector machine (SVM), which aims to find a line or a surface so that all training set samples fall on the line and surface as much as possible (Douha, Benoudjit, Douak, & Melgani, 2012). The model is mostly used for prediction under nonlinear conditions, and has the advantages of excellent generalization performance, global convergence, and insensitivity to sample dimensionality (Liu, Jiang, & Chen, 2022). Applying the SVR model to nonlinear regression involves mapping the feature vectors of the low-dimensional space into a higher dimensionality, so it is necessary to build a mapping function to expand the dimension, and at the same time introduce the libSVM toolkit to select kernel functions to reduce the computational cost.

The radial basis function (RBF) was selected as the kernel function in this study. The grid search method was utilized to optimize the penalty parameter C and the RBF kernel function's parameter g, as part of establishing the optimal regression model with the SVR. The search range was $[2^{-10}, 2^{10}]$ and the search steps were all 0.5.

2.4.6. Model evaluation

In this study, the determination coefficient of prediction (R_P^2) and the RMSEP were utilized to upgrade the input feature variables of the model

Table 1
Statistics of rapeseed oil procymidone concentrations in the training and prediction set.

Subsets	Number of samples	Units	Maximum	Minimum	Mean	Standard deviation
Training set	111	mg•kg^{-1}	100	0.1	11.5788	25.5833
Prediction set	31	mg•kg^{-1}	100	0.1	12.2952	26.3628

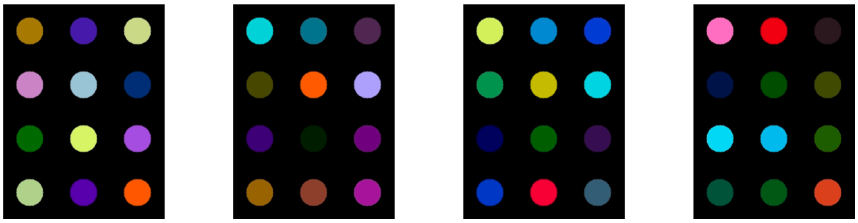

Fig. 2. The difference image of sensor array with different concentrations of pesticide residues.

and evaluate the generalization performance of the established SVR model. Below are the specific formulas used in this study:

$$\mathrm{RMSEP} = \sqrt{\frac{\sum_{i=1}^{n_p}(y_i - y_i^{'})^2}{n_p}} \quad (1)$$

$$\mathrm{R_P^2} = 1 - \frac{\sum_{i=1}^{n_p}(y_i - y_i^{'})^2}{\sum_{i=1}^{n_p}(y_i - y_p^{''})^2} \quad (2)$$

where, y_i represents the actual procymidone concentrations value of the i-th rapeseed oil sample, $y_i^{'}$ represents the prediction value of the i-th rapeseed oil sample, $y_p^{''}$ represents the average of the predicted values of the test set samples. n_p represents the specific number of samples used in the test set for this study.

2.5. Software

MATLAB R2021a (MathWorks, Natick, USA) running on Windows 10 was utilized to implement all algorithms in this study.

3. Results and discussion

3.1. Sample division

In this study, the 142 rapeseed oil samples obtained in the experiment were separated into training and prediction sets with a 7:2 ratio, and 111 training set samples and 31 prediction set samples were acquired, respectively. Table 1 shows the statistics of rapeseed oil procymidone concentrations in the training set and the prediction set. Analysis of Table 1 indicates that both the training and prediction sets have small mean and standard deviation values. Therefore, the division of samples is reasonable and can be used for model training.

3.2. Response results of sensor array

Fig. 2 displays the variation in images of the sensor array across different concentrations of procymidone residues in rapeseed oil samples. Fig. 2 clearly displays the obtained results that there are obvious differences in the characteristic images of rapeseed oil samples with different concentrations of procymidone residues. This is due to the difference in the composition and concentration of volatile gases produced by rapeseed oil samples with different concentrations, resulting in some differences in the characteristic image after its reaction with chemical dyes.

3.3. Results of PSO algorithm optimizing feature

Fig. 3 displays the results of the PSO algorithm optimizing the characteristics of sensor. Fig. 3A demonstrates the selection of various characteristic color components using the PSO algorithm results.

As evident from Fig. 3A, when 12 variables with characteristics are selected, the $\mathrm{R_P^2}$ is the largest, which is 0.9643, and the RMSEP value is 4.5934 mg • kg^{-1}. Therefore, 12 characteristic color combinations were selected as the best solution. Fig. 3B shows the result of each optimization feature variable of the PSO-SVR model running independently 50 times. From Fig. 3B, it can be calculated that the mean $\mathrm{R_P^2}$ is 0.8966 and the mean RMSEP is 8.1847 mg • kg^{-1}.

3.4. Results of GA optimizing feature

Fig. S1 displays the results of the GA algorithm optimizing the color characteristics of the sensor. Fig. S1A demonstrates the selection of various characteristic color components using the GA results. As evident from Fig. S1A, when 7 variables with characteristics are selected, the $\mathrm{R_P^2}$ is the largest, which is 0.9794, and the RMSEP value is 3.9443 mg • kg^{-1}. Therefore, 7 characteristic color combinations were selected as the best solution. Fig. S1B shows the result of each optimization feature variable of the GA-SVR model running independently 50 times. From Fig. S1B, it can be calculated that the mean $\mathrm{R_P^2}$ is 0.9104 and the mean RMSEP is 7.6185 mg • kg^{-1}.

3.5. Results of ACO algorithm optimizing feature

Fig. S2 displays the results of the ACO algorithm optimizing the color characteristics of the sensor. Fig. S2A demonstrates the selection of various characteristic color components using the ACO results. As evident from Fig. S2A, when 12 variables with characteristics are selected, the $\mathrm{R_P^2}$ is the largest, which is 0.9787, and the RMSEP value is 4.8310 mg • kg^{-1}. Therefore, 12 characteristic color combinations were selected as the best solution. Fig. S2B shows the result of each optimization feature variable of the ACO-SVR model running independently 50 times. From Fig. S2B, it can be calculated that the mean $\mathrm{R_P^2}$ is 0.8965 and the mean RMSEP is 8.1632 mg • kg^{-1}.

3.6. Results of SA optimizing feature

Fig. S3 displays the results of the SA algorithm optimizing the color characteristics of the sensor. Fig. S3A demonstrates the selection of various characteristic color components using the SA results. As evident from Fig. S3A, when 13 variables with characteristics are selected, the

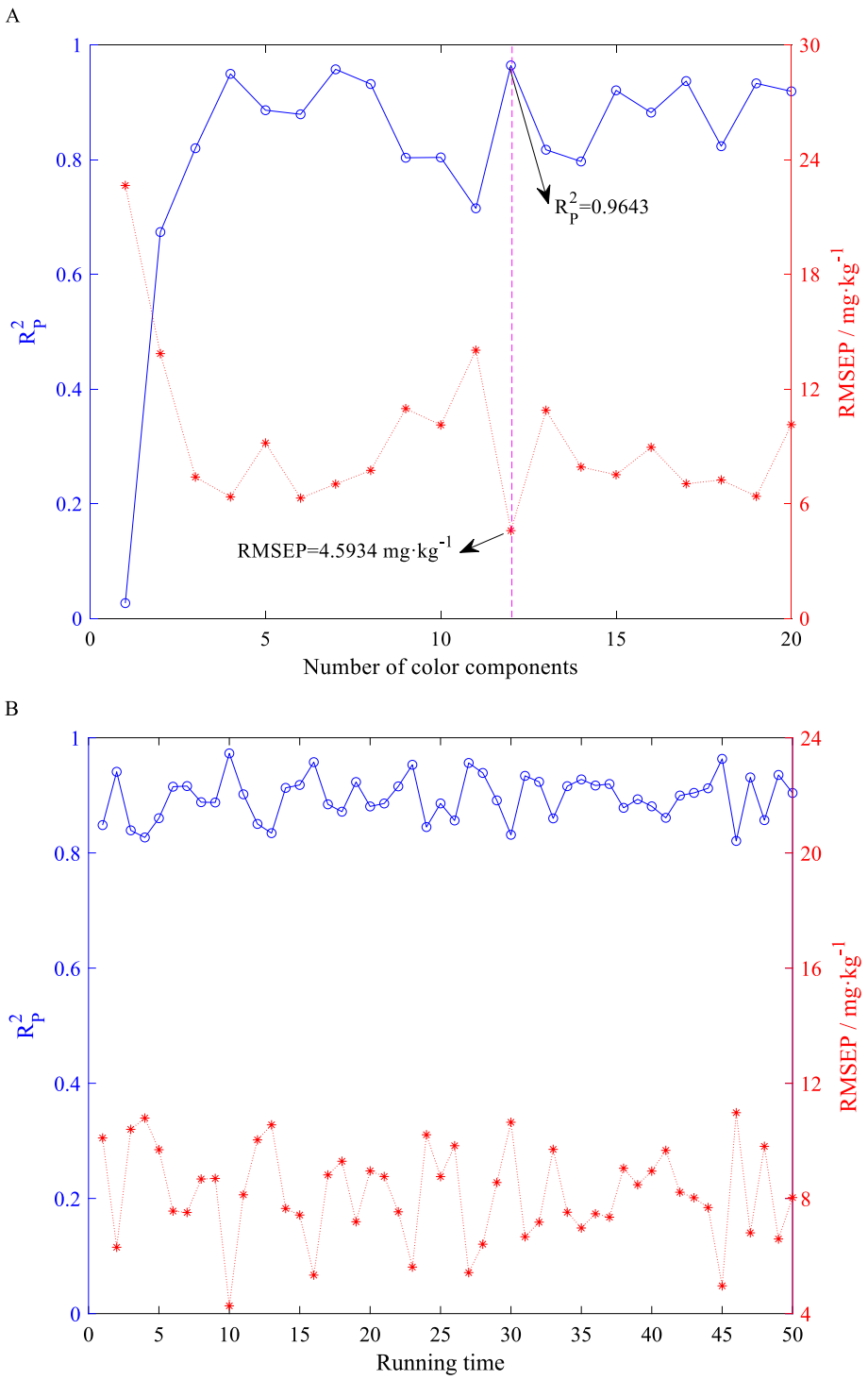

Fig. 3. Results of different number of color features by PSO algorithm and results of each optimization feature variable of the PSO-SVR model running independently 50 times.

RMSEP value is the smallest, which is 5.7315 mg • kg^{-1}, and R_P^2 is 0.9338. Therefore, 13 characteristic color combinations were selected as the best solution. Fig. S3B shows the result of each optimization feature variable of the SA-SVR model running independently 50 times. From Fig. S3B, it can be calculated that the mean R_P^2 is 0.9063 and the mean RMSEP is 7.7496 mg • kg^{-1}.

3.7. Result of SVR model with different components

Table 2 illustrates the best prediction results of SVR models based on different combinations of input characteristic variables. Table 2 reveals the following observations that the training effect and prediction results of SVR models are significantly improved by optimizing the input feature variables. Compared with the SVR model, the SA-SVR model based on C = 32.0000 and g = 0.5000 had the best training effect and prediction results, and its R_C^2 increased from 0.8759 to 0.9878, and

Table 2
The best results of SVR models based on different combinations of input characteristic variables.

Models	Number of features	Parameters	R_C^2	RMSEC/ mg•kg^{-1}	R_P^2	RMSEP/ mg•kg^{-1}
SVR	36	C = 8.0000, g = 0.0313	0.8759	8.9938	0.8285	10.7679
PSO-SVR	12	C = 22.6274, g = 0.5000,	0.9821	3.4353	0.9729	4.2700
GA-SVR	7	C = 5.6569, g = 1.4142	0.9647	4.7958	0.9646	4.8793
ACO-SVR	12	C = 22.6274, g = 0.3536	0.9730	4.1754	0.9713	4.3929
SA-SVR	13	C = 32.0000, g = 0.5000	0.9878	2.7432	0.9894	2.6679

RMSEC decreased from 8.9938 mg • kg^{-1} to 2.7432 mg • kg^{-1}. The R_P^2 of the model showed an increase from 0.8285 to 0.9894, and the RMSEP went down from 10.7679 mg • kg^{-1} to 2.6679 mg • kg^{-1}.

Further analysis from Table 2 shows that the GA-SVR model has the lowest number of input features and the SVR model has the largest number of input features, but their prediction results are not as good as those of PSO-SVR, ACO-SVR, SA-SVR models. It may be that there are too many input feature points selected by SVR model, and some of them are irrelevant, resulting in a large deviation in the final result. However, the number of input features selected by the GA-SVR model is small, and the selected feature points cannot represent the entire data, and a small number of key data is lost, resulting in poor final results. Therefore, when selecting the number of input features, it is necessary to remove redundant and invalid feature points, reduce data complexity, and retain highly targeted feature points.

4. Conclusions

This study verifies the feasibility of quantitative analysis of procymidone concentration in rapeseed oil by olfactory visualization technology. Four intelligent optimization algorithms (i.e., PSO, GA, ACO, SA) are used separately to upgrade the features of a sensor array, and SVR models based on different optimization features are established. The results show that the performances of SVR models based on optimized features are improved to a certain extent. Among them, the SA-SVR model has the best prediction effect. From this, we can infer that olfactory visualization technology combined with multivariate analysis will have a good application prospect in the quantitative analysis of edible oil pesticide residues.

Declaration of Competing Interest

The authors declare that they have no known competing financial interests or personal relationships that could have appeared to influence the work reported in this paper.

Data availability

Data will be made available on request.

Acknowledgements

The authors gratefully acknowledge the financial support provided by the National Key Research and Development Program of China (Grant No. 2017YFC1600603).

Appendix A. Supplementary data

Supplementary data to this article can be found online at https://doi.org/10.1016/j.fochx.2023.100794.

References

Chen, Z.-L., Dong, F.-S., Xu, J., Liu, X.-G., & Zheng, Y.-Q. (2015). Management of pesticide residues in China. *Journal of Integrative Agriculture, 14*(11), 2319–2327.
Ding, L.-N., Li, T., Guo, X.-J., Li, M., Liu, X.-Y., Cao, J., & Tan, X.-L. (2021). Sclerotinia stem rot resistance in rapeseed: Recent progress and future prospects. *Journal of Agricultural and Food Chemistry, 69*(10), 2965–2978.
Douha, L., Benoudjit, N., Douak, F., & Melgani, F. (2012). Support vector regression in spectrophotometry: An experimental study. *Critical Reviews in Analytical Chemistry, 42*(3), 214–219.
Garcia-Febrero, R., Salvador, J. P., Sanchez-Baeza, F., & Marco, M. P. (2014). Rapid method based on immunoassay for determination of paraquat residues in wheat, barley and potato. *Food Control, 41*, 193–201.
Hird, S. J., Lau, B. P. Y., Schuhmacher, R., & Krska, R. (2014). Liquid chromatography-mass spectrometry for the determination of chemical contaminants in food. *Trac-Trends in Analytical Chemistry, 59*, 59–72.
Jiang, H., Liu, T., He, P., & Chen, Q. (2020). Quantitative analysis of fatty acid value during rice storage based on olfactory visualization sensor technology. *Sensors and Actuators B-Chemical, 309*.
Jiang, H., Liu, T., He, P., Ding, Y., & Chen, Q. (2021). Rapid measurement of fatty acid content during flour storage using a color-sensitive gas sensor array: Comparing the effects of swarm intelligence optimization algorithms on sensor features. *Food Chemistry, 338*.
Jiang, H., Xu, W., & Chen, Q. (2019a). Comparison of algorithms for wavelength variables selection from near-infrared (NIR) spectra for quantitative monitoring of yeast (Saccharomyces cerevisiae) cultivations. *Spectrochimica Acta Part a-Molecular and Biomolecular Spectroscopy, 214*, 366–371.
Jiang, H., Xu, W., & Chen, Q. (2019b). Evaluating aroma quality of black tea by an olfactory visualization system: Selection of feature sensor using particle swarm optimization. *Food Research International, 126*.
Jordehi, A. R. (2014). Particle swarm optimisation for dynamic optimisation problems: A review. *Neural Computing & Applications, 25*(7–8), 1507–1516.
Katsoudas, E., & Abdelmesseh, H. H. (2000). Enzyme inhibition and enzyme-linked immunosorbent assay methods for carbamate pesticide residue analysis in fresh produce. *Journal of Food Protection, 63*(12), 1758–1760.
Liu, S., Fu, L., Hai, F., Jiang, J., Che, Z., Tian, Y., & Chen, G. (2018). Sensitivity to boscalid in field isolates of Sclerotinia sclerotiorum from rapeseed in Henan Province, China. *Journal of Phytopathology, 166*(4), 227–232.
Liu, T., He, J., Yao, W., Jiang, H., & Chen, Q. (2022). Determination of aflatoxin B1 value in corn based on Fourier transform near-infrared spectroscopy: Comparison of optimization effect of characteristic wavelengths. *LWT-Food Science and Technology*, 164.
Liu, T., Jiang, H., & Chen, Q. (2020). Qualitative identification of rice actual storage period using olfactory visualization technique combined with chemometrics analysis. *Microchemical Journal, 159*.
Liu, T., Jiang, H., & Chen, Q. (2022). Input features and parameters optimization improved the prediction accuracy of support vector regression models based on colorimetric sensor data for detection of aflatoxin B_1 in corn. *Microchemical Journal, 178*.
Mao, W., & Jiang, H. (2022). Determination of ethanol content during simultaneous saccharification and fermentation (SSF) of cassava based on a colorimetric sensor technique. *RSC Advances, 12*(7), 3996–4004.
Mohan, B. C., & Baskaran, R. (2012). A survey: Ant Colony Optimization based recent research and implementation on several engineering domain. *Expert Systems with Applications, 39*(4), 4618–4627.
Niazi, A., & Leardi, R. (2012). Genetic algorithms in chemometrics. *Journal of Chemometrics, 26*(6), 345–351.
Rakow, N. A., & Suslick, K. S. (2000). A colorimetric sensor array for odour visualization. *Nature, 406*(6797), 710–713.
Sanaeifar, A., Li, X., He, Y., Huang, Z., & Zhan, Z. (2021). A data fusion approach on confocal Raman microspectroscopy and electronic nose for quantitative evaluation of pesticide residue in tea. *Biosystems Engineering, 210*, 206–222.
Shen, J., Liu, Y., Wang, X., Bai, J., Lin, L., Luo, F., & Zhong, H. (2023). A comprehensive review of health-benefiting components in rapeseed oil. *Nutrients, 15*(4).
Suman, B., & Kumar, P. (2006). A survey of simulated annealing as a tool for single and multiobjective optimization. *Journal of the Operational Research Society, 57*(10), 1143–1160.
Suslick, K. S., Rakow, N. A., & Sen, A. (2004). Colorimetric sensor arrays for molecular recognition. *Tetrahedron, 60*(49), 11133–11138.
Tang, X., Xiao, W., Shang, T., Zhang, S., Han, X., Wang, Y., & Sun, H. (2020). An electronic nose technology to quantify pyrethroid pesticide contamination in tea. *Chemosensors, 8*(2).

Tang, Y., Xu, K., Zhao, B., Zhang, M., Gong, C., Wan, H., … Yang, Z. (2021). A novel electronic nose for the detection and classification of pesticide residue on apples. *RSC Advances, 11*(34), 20874–20883.

Xu, W., He, Y., Li, J., Deng, Y., Zhou, J., Xu, E., … Liu, D. (2022). Olfactory visualization sensor system based on colorimetric sensor array and chemometric methods for high precision assessing beef freshness. *Meat Science, 194*.

Zhu, C., Deng, J., & Jiang, H. (2022). Parameter optimization of support vector machine to improve the predictive performance for determination of aflatoxin B_1 in peanuts by olfactory visualization technique. *Molecules, 27*(19).